Electronic Supplementary Material (ESI) for Green Chemistry.

Supplementary Information

Facile In-Situ Construction of Covalent Adaptable Network in Polyester Vitrimer for Advanced Performance in Repairability, Foamability and Recyclability

Pengzhi Li[a], Bin Lan[a], Xutao Zhang[a,b], Siyuan Lei [a], Qi Yang*[a], Pengjian Gong*[a], Chul B. Park[a,c] and Guangxian Li[a]

a. *College of Polymer Science and Engineering, State Key Laboratory of Polymer Materials Engineering, Sichuan University, 24 Yihuan Road, Nanyiduan, Chengdu, Sichuan, People's Republic of China, 610065*
b. *Jiangsu JITRI Advanced Polymer Materials Research Institute, Tengfei Building, 88 Jiangmiao Road, Jiangbei New District, Nanjing, Jiangsu, 211800, People's Republic of China*
c. *Microcellular Plastics Manufacturing Laboratory, Department of Mechanical and Industrial Engineering, University of Toronto, 5 King's College Road, Toronto, Ontario, Canada M5S 3G8*

* Corresponding authors: Qi Yang. Email address: yangqi@scu.edu.cn. Tel: +028-8540-5402

* Corresponding authors: Pengjian Gong. Email address: pgong@scu.edu.cn. Tel: +028-8540-1841

Contents

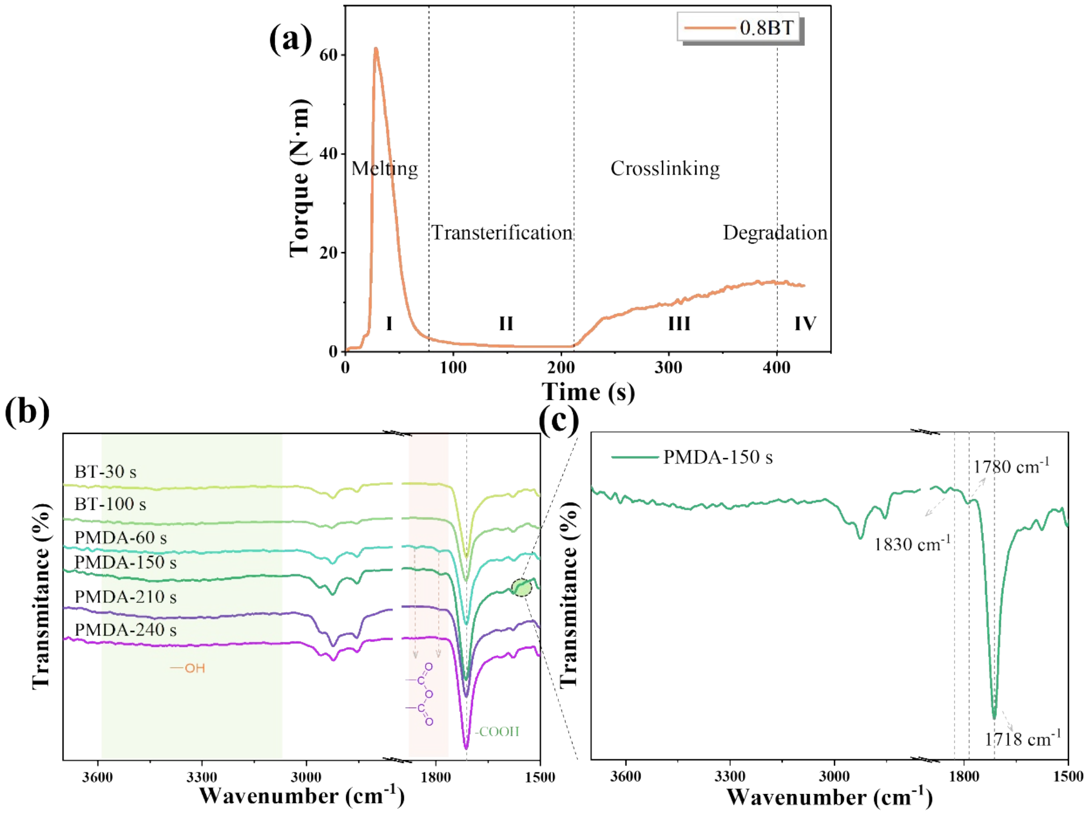

Figure S1. (a)Torque-time curve of sample 0.8 BT, (b)FTIR curves of 0.8BT at different synthesis time, (c) enlargement of PMDA-90 s curve. Sample is named by the combination of additive and the corresponding time of sample with related additive being taken out. For example, BT-30 s means the sample that was taken out after BIS-TRIS being added in the internal mixer for 30 s.

Figure S1 is torque-time curve of sample 0.8BT. In the first stage, PET and BIS-TRIS was added into inter mixer and then gradually melted under high temperature and shearing, resulting in the presence of torque peak. In the second sage, BIS-TRIS embedded into PET chains though transesterification. The reactions shorten PET chains, and hence further decreased the torque. when the curve reached a plateau, it was believed BIS-TRIS had been fully embedded into PET chains. In the third stage, PMDA was added into inter mixer. Due to the fast-crosslinking reactions, toque quickly increased and then reached the second plateau when crosslinking reaction were complete. In the fourth stage, torque gradually decreased due to the gradation.

The reactions occurred in the internal mixer were further studied on polymer obtained at different reaction times by FTIR as shown in Figure S1(b, c). It is noted that all FTIR curves have a characteristic broaden peak of hydroxyl group around ~ 3500 cm^{-1}, indicating the existing of hydroxyl groups even after the reactions finishing. The characteristic double peaks around ~ 1780 cm^{-1} ~ 3500 cm^{-1} of anhydride groups from PMDA are observed in FTIR curves of sample PMDA-60 s and sample PMDA-150s, while disappeared in sample PMDA-210s and sample PMDA-240s. The phenomenon suggests that the crosslinking reactions between anhydride groups and hydroxyl groups are completed in 210 s after PMDA added in the internal mixer. The peak at ~ 1718 cm^{-1} is ascribed to carboxyl groups. It is noted that the peak strength of sample PMDA-240s is significantly higher than that of sample PMDA-210s, ascribing to ester groups' degradation which would generate carboxyl groups at high temperature (higher than 270 ℃) and shearing conditions. The FTIR results are highly consistent with the torque curve, both of which clarify the reaction process and could instruct the synthesis of PET-based vitrimer.

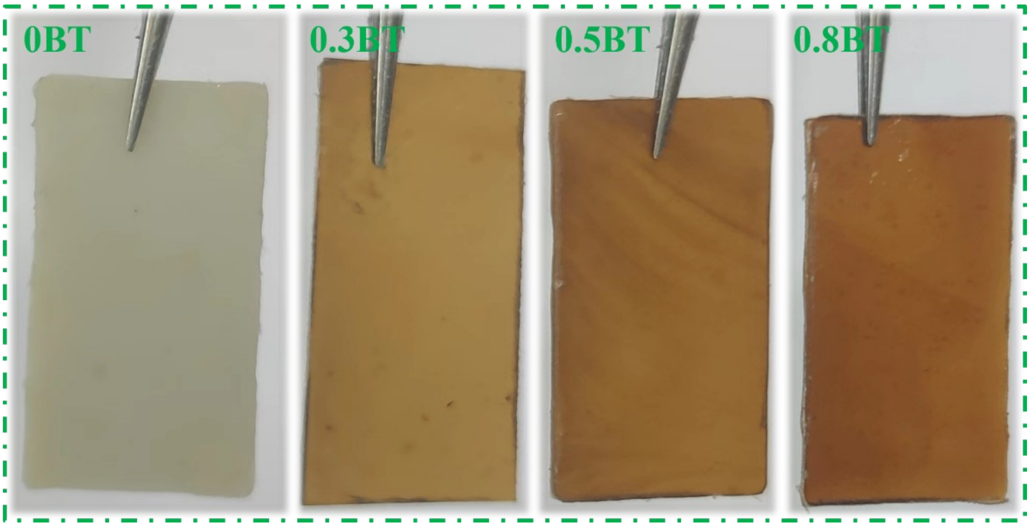

Figure S2. Photographs of 0 BT to 0.8 BT.

All samples were hot pressed at 270℃ and 10 MPa after processing and presented as Figure S2.

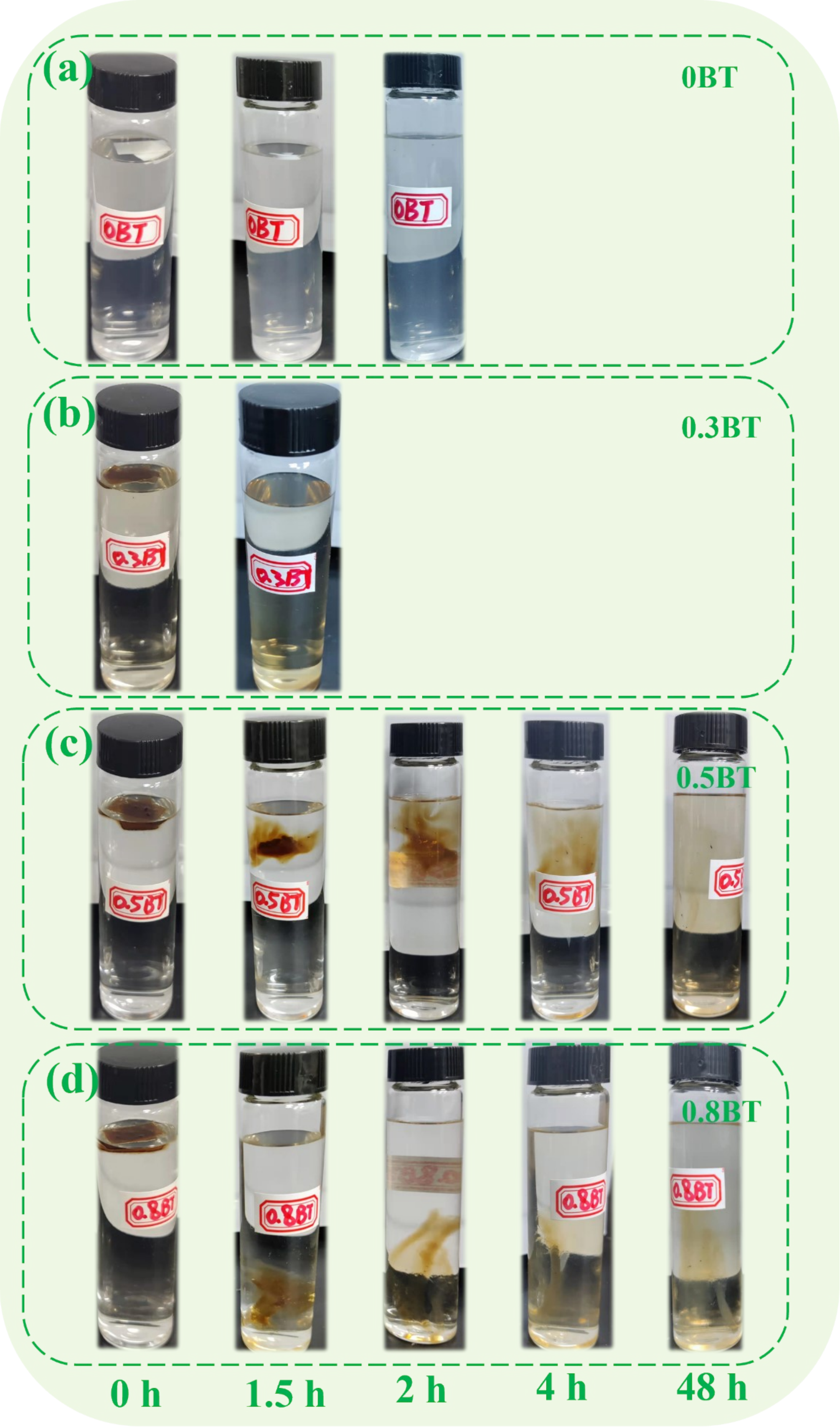

Figure S3. Swelling tests of different samples: (a) 0 BT, (b) 0.3 BT, (c) 0.5 BT, (d) 0.8 BT.

The swelling test demonstrated the generation of crosslinking structure in samples 0.5 BT and 0.8 BT, while not generated in samples 0 BT and 0.3 BT as shown in Figure S3. It was speculated that 0.8 BT had denser crosslinking structure than 0.5 BT, while 0.8 BT had smaller swell ratio as Figure S4 presented.

Figure S4. Morphologies of cross-linked samples after swelling in TFA.

Figure S5 presented the stress relaxation curves of 0.8 BT at different temperature, which implied that 0.8 BT could totally relax in the temperature range.

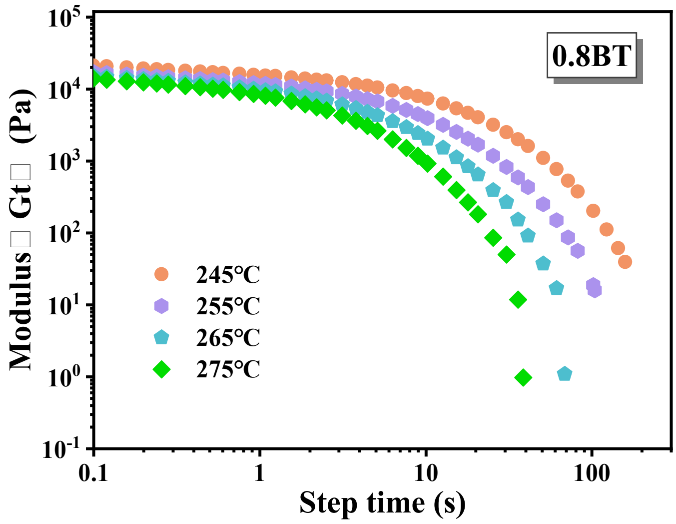

Figure S5. Stress relaxation curves of 0.8 BT at different temperature.

Figure S8 shows that 0.8 BT and 0.5 BT had obvious strain-hardening behavior, ascribing to the crosslinking network.

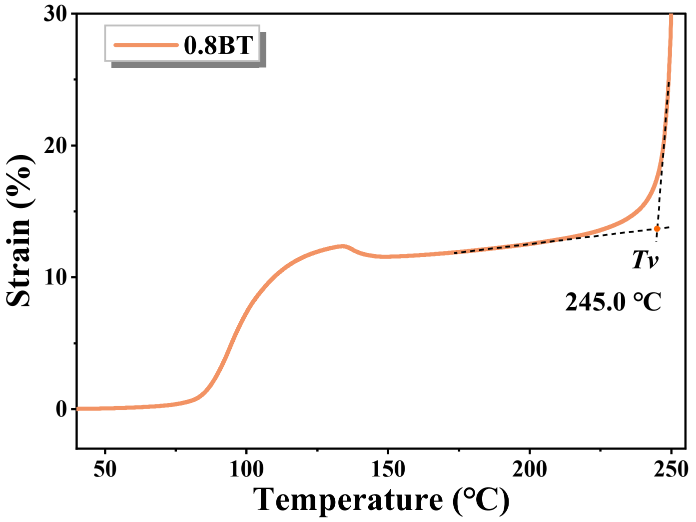

Figure S6. Volume expansion curve of o.8BT.

Figure S6. is the Volume expansion curve of o.8BT from DMA. T_v was calculated as 245 °C, at where strain increased dramatically.

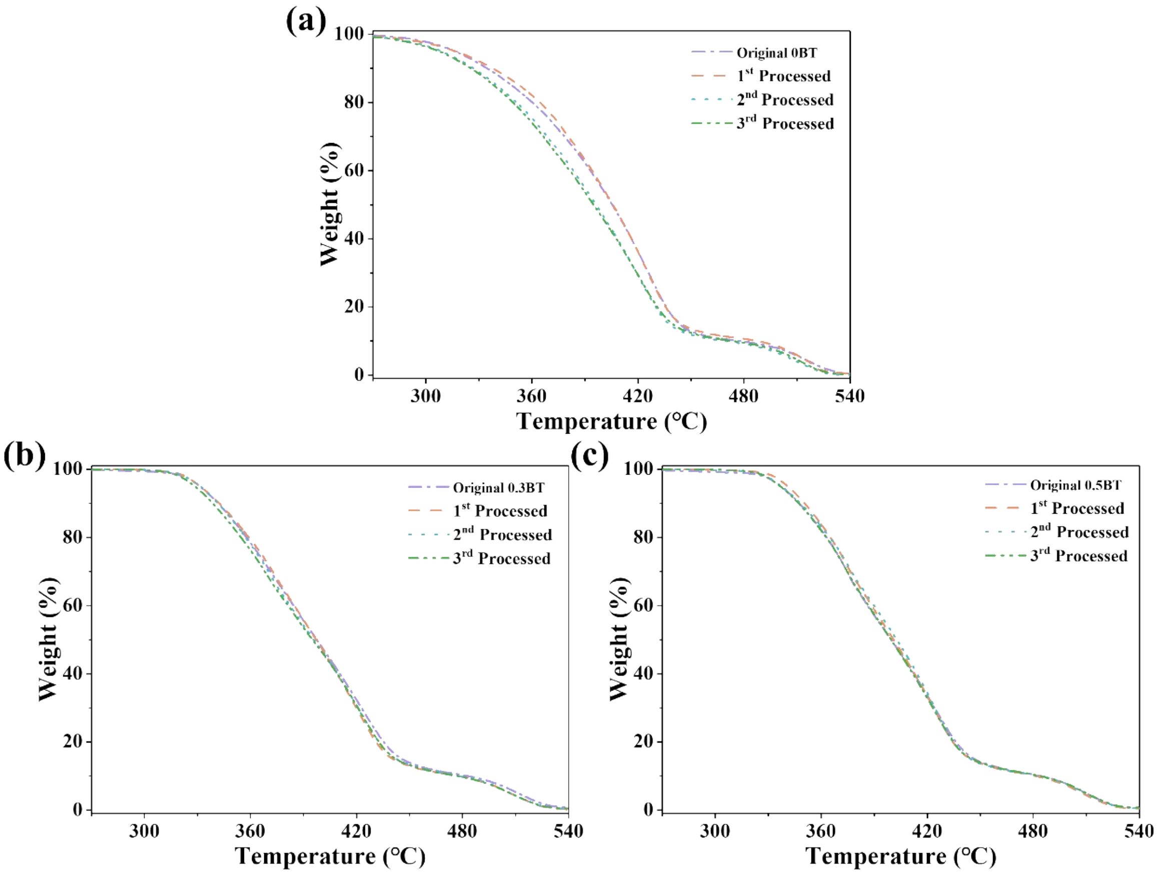

Figure S7. TG curves of sample 0.3 BT,0 BT, and 0.8 BT after reprocessing, respectively.

TG curves of sample 0.3 BT,0 BT, and 0.8 BT after reprocessing are presented in Figure S7. For sample 0 BT that does not have covalent adaptable networks, the thermal stability was decreased significantly after multiple reprocessing as shown in Figure S7(a). As for sample 0.3 BT and sample 0.5 BT, samples' thermal stability was gradually increased with increasing BIS-TRIS content. Compared with sample 0 BT, sample 0.8 BT processes much better thermal stability after reprocessing as shown in Fig 6c, ascribing to (1) consumption of carboxyl groups by hydroxyl groups (residual carboxyl group deteriorates thermal stability); (b) formation of cross-linked networks (cross-linked network enhances thermal stability).

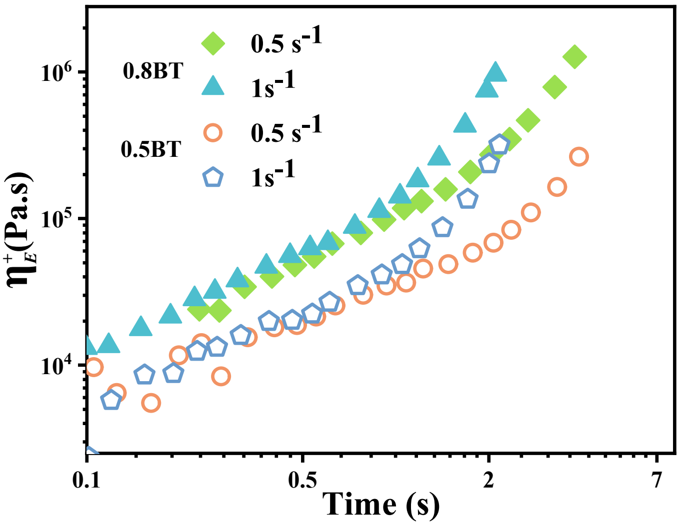

Figure S8. Extensional rheological behaviors of 0.8 BT and 0.5 BT

Figure S9 indicates the crosslinking structure decreases melting point of PET, which had the effect on crystalline temperature as Figure S10 presents, both resulted from the restriction of chain mobility.

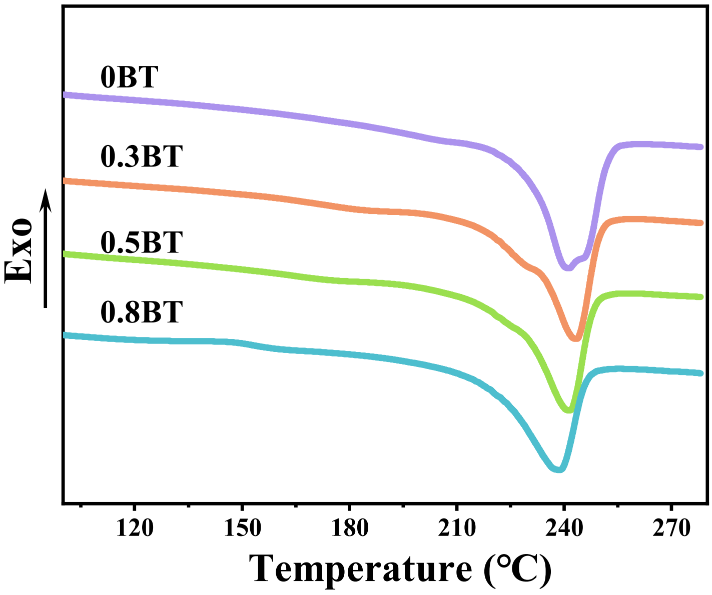

Figure S9. Melting behavior of different samples.

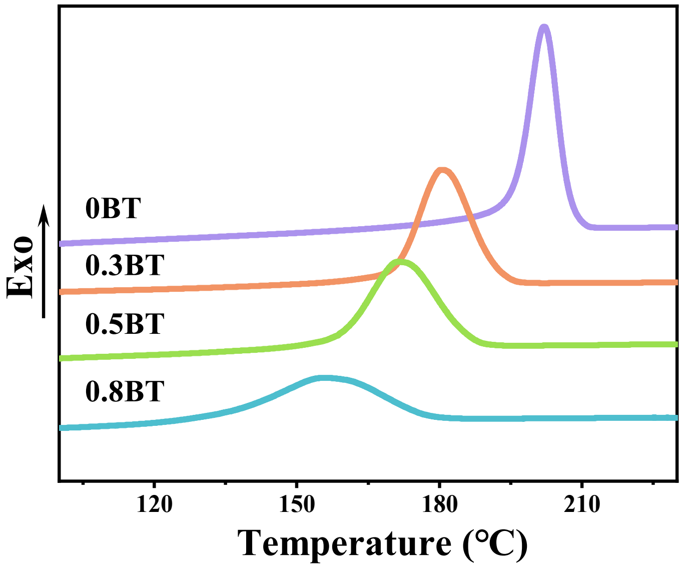

Figure S10 Crystallization behavior of different samples.

Figure S11 indicates crosslinking structure helps to increase thermal stability of PET.

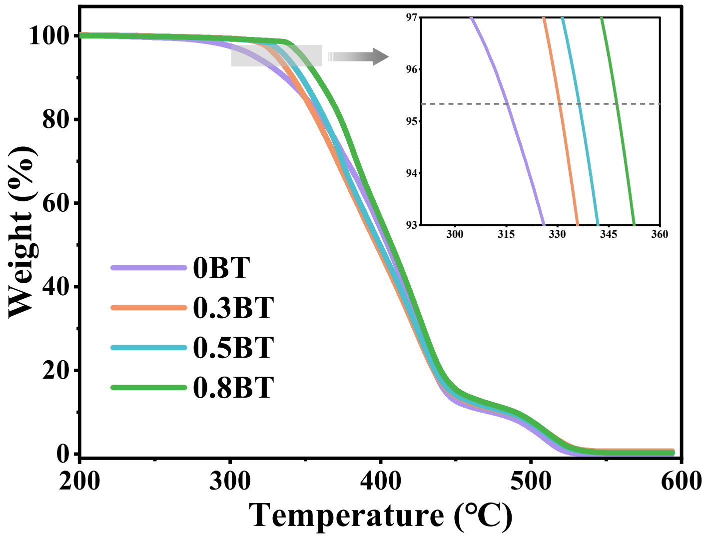

Figure S11 Thermogravimetric curves of different samples.

Figure S12 indicates 0.8 BT foam had uniform foam morphology with closed cell structure.

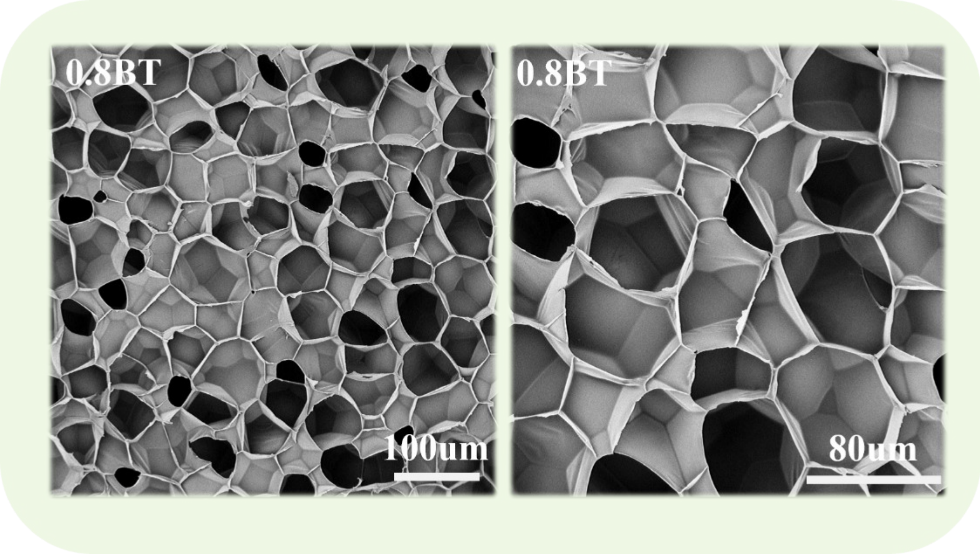

Figure S12. Foam morphology of sample 0.8 BT.